Soil & Tillage Research 179 (2018) 71–81

Contents lists available at ScienceDirect

Soil & Tillage Research

journal homepage: www.elsevier.com/locate/still

Spatial analysis of soil aggregate stability in a small catchment of the Loess Plateau, China: I. Spatial variability

Luping Ye[a,c], Wenfeng Tan[a,b,c,*], Linchuan Fang[a], Lingling Ji[b], Huang Deng[b]

[a] State Key Laboratory of Soil Erosion and Dryland Farming on the Loess Plateau, Institute of Soil and Water Conservation, Chinese Academy of Sciences and Ministry of Water Resources, Yangling 712100, China

[b] Key Laboratory of Arable Land Conservation (Middle and Lower Reaches of Yangtze River), Ministry of Agriculture, Huazhong Agricultural University, Wuhan 430070, China

[c] University of Chinese Academy of Sciences, Beijing 100049, China

ARTICLE INFO

Keywords:
Soil aggregate stability
Soil erodibility
Spatial analysis

ABSTRACT

The intrinsic and extrinsic factors that control soil aggregate formation have been widely studied at the aggregate scale, but little is known about their roles in aggregate formation at different landscape scales. Here, a spatial analysis of soil aggregate stability and erodibility (K factors) was performed to understand the formation processes of aggregates at catchment scale. Spatial structures of the mean weight-diameter (MWD, mm), water-stable aggregates greater than 0.25 mm ($WSA_{>0.25}$, %) and K factors were investigated by using classical statistics, semivariograms, Local Indicators of Spatial Association (LISA), spatial interpretation, and spatial overlay in a small catchment of the Loess Plateau, China (LPC). The results showed that MWD and $WSA_{>0.25}$ were significantly lower in farmland than in other land types, and were obviously higher in shrubland than in woodland, but it was the opposite case for K factors. Nugget/sill ratios $C_0/(C_0 + C)$ showed a very strong spatial dependence for MWD (9.13% at 0–10 cm and 19.49% at 10–20 cm soil layer) and $WSA_{>0.25}$ (12.48% at 0–10 cm and 17.71% at 10–20 cm soil layer). These data and LISA results implied that the spatial variability of MWD, $WSA_{>0.25}$ and K factors in the Zhifanggou catchment was mainly controlled by intrinsic factors such as parent materials, terrain attributes and soil types. Besides, the effects of extrinsic factors (land use and farming practice) could not be ignored, especially for K factors. Cross-validation results illustrated that ordinary kriging (OK) performed better than inverse distance weighting (IDW) for MWD and $WSA_{>0.25}$, but it was the opposite for K factors as a whole. Land-use type, topography, vegetation, and revegetation duration showed interactive effects on the spatial heterogeneity of soil aggregate stability and K factors. Spatial analysis showed great potential to be applied in the analysis of the influencing factors of soil aggregate stability at the small catchment scale.

1. Introduction

Soil aggregates are the basic units of soil structure, and their stability is critical for soil water movement and storage, fertility, aeration, erosion, carbon sequestration, biological activity, and root penetration (Algayer et al., 2014a; Amezketa, 1999; Gallardo-Carrera et al., 2007; Deng et al., 2014; Jastrow and Miller, 1997; Lynch and Bragg, 1985; O'Brien and Jastrow, 2013). Soil aggregate stability and erodibility K factors are often used as the key indices to evaluate soil degradation or soil erodibility (Algayer et al., 2014b; Shi et al., 2012). The large spatial variability of aggregate stability and K factors is inherent because of geologic and pedologic soil forming factors, and a part of this variability may result from agricultural management or human disturbance. Therefore, digital mapping of soil aggregate stability and K factors is significant for the evaluation of soil erosion, and analysis of their spatial heterogeneity may facilitate a understanding of the aggregate formation processes and the reasons for their spatial differences (Cambardella et al., 1994; Castrignanò et al., 2000).

Classical statistics (Cantón et al., 2009; Hajabbasi and Hemmat, 2000) and geostatistics (Cambardella et al., 1994; Castrignanò et al., 2000) are generally used to study the spatial heterogeneity of aggregate stability and soil erodibility. Classical statistics requires some basic hypotheses, such as the spatial independence of variables, which may produce erroneous or misleading results (Nielsen and Alemi, 1989). Conversely, geostatistics was established based on the theory of regionalized variables, considering the spatial dependence of variables. It enables the

* Corresponding author at: Key Laboratory of Arable Land Conservation (Middle and Lower Reaches of Yangtze River), Ministry of Agriculture, College of Resources and Environment, Huazhong Agricultural University, Wuhan 430070, China.

E-mail addresses: yeluping1991@yahoo.com (L. Ye), wenfeng.tan@hotmail.com (W. Tan), jilingling_2015@hotmail.com (L. Ji), denghuang@webmail.hzau.edu.cn (H. Deng).

https://doi.org/10.1016/j.still.2018.01.012
Received 10 May 2017; Received in revised form 12 January 2018; Accepted 30 January 2018
Available online 10 February 2018
0167-1987/

analysis, assessment and interpretation of the spatial structures of regional variables, and the prediction of variables at unknown locations.

In recent years, more and more studies of spatial variability in soil properties have been performed by geostatistics (Cambardella et al., 1994; Freitas et al., 2015; Júnior et al., 2006; Ou et al., 2017). However, research on the spatial patterns of aggregate stability is limited (Castrignanò et al., 2000; Castrignanò and Stelluti, 1999; Shukla et al., 2007; Siqueira et al., 2010) compared with that on other soil properties, such as soil texture (Langella et al., 2016; Wang and Shi, 2017), soil moisture (Júnior et al., 2006) and soil organic carbon content (SOC) (Annabi et al., 2017). Cambardella et al. (1994) analyzed the spatial distributions of different soil variables at two sites within a catchment in central Iowa and suggested that spatial relationships were comparable within the similar landscapes. Barik et al. (2014) determined the effects of traffic compaction on the changes in spatial variability of soil properties and showed that aggregate stability is significantly affected by traffic operation. Current literatures about the spatial variability of aggregate stability ignore the local spatial autocorrelation and the local clusters of similar behavior in the spatial arrangement. Besides, these studies have confirmed the important effects of environmental factors such as topography, land use and vegetation on the heterogeneity of aggregate stability and soil erodibility at different spatial scales. However, their interactive effects remain unclear.

The Loess Plateau of China (LPC) covers an area of 640,000 km^2 in northwestern China, and is recognized as the most eroded landscapes in the world. The soil of LPC was developed from loess deposits (Wang et al., 2017). A unique combination of climate, topography, vegetation factor, soil property, and unsustainable agricultural practices leads to severe soil erosion (Zhang, 1991). The severe soil erosion can be effectively prevented by afforestation, but it is still severe in cultivated slope farmland (Zhang et al., 2008). Then the "Grain for Green" project (GGP) was implemented in 1999 to restore the fragile ecosystems by converting the slope farmland and wasteland into grassland, shrubland and woodland (Zhou et al., 2012). The significant achievements of GGP in controlling soil erosion have been widely acknowledged. However, little is known about the spatial distribution of soil erosion resistance on LPC. Hence, it is necessary to understand the spatial variability and spatial autocorrelation of aggregate stability and soil erodibility on LPC. The Zhifanggou catchment, which is located at the center of LPC, is a typical hilly gullied loess landscape, and its soil was derived from wind-accumulated loess parent material and has a vertically and laterally uniform silt loam texture. After 30 years of ecological restoration supported by the Chinese Academy of Sciences, the Zhifanggou catchment has become a popular catchment for understanding the soil and water conservation on LPC (Wang et al., 2011; Zhao et al., 2017; Zhao et al., 2016; Zhou et al., 2006). Several practical revegetation methods have been applied at different times since the 1980s, making the Zhifanggou catchment an appropriate environment for studying the intrinsic and extrinsic factors that control the soil aggregate formation. In addition, abundant basic data about Zhifanggou catchment are available, providing an excellent data platform for furture research such as the National Earth System Science Data Sharing Infrastructure, http://loess.geodata.cn.

The present study was aimed to (1) analyze the variation of aggregate stability and soil erodibility under different land-use types and identify the reasons based on the aggregate size distribution by classical statistics, (2) evaluate how spatial variability of aggregate stability and K factors are affected by land-use types, vegetation, topography, and revegetation at the local spatial scale, and (3) how these factors determine their spatial distributions by semivariograms, Local Indicators of Spatial Association (LISA), and spatial interpretation.

2. Materials and methods

2.1. Study area and soil sampling

Zhifanggou catchment is located at the Ansai Research Station of Soil and Water Conservation in Shaanxi Province in the center of LPC. It is a typical catchment in the hilly gullied loess landscape with slopes varying from 0° to 65° (109°13′03″ – 109°16′46″ E longitude, 36°46′28″ – 36°46′42″ N latitude, 1010 – 1431 m altitude, 8.27 km^2) (Fig. 1a, b). The climate is typically semiarid with a mean annual temperature of 8.8 °C (−23.6 °C to 36.8 °C). Its average annual precipitation is about 505 mm and falls between July and September with over 60% precipitation. The soil is mainly Orthic Entisol according to Chinese Soil Taxonomy (Cooperative Research Group on Chinese Soil Taxonomy (CRGCST, 2001) or Calcaric Regosols according to WRB reference system (IUSS Working Group WRB, 2014), and was derived from wind-accumulated loess parent material with an average thickness of 50–80 m. The soil is of a uniform silt loam texture, and the average sand, silt and clay contents are 21 ± 6%, 63 ± 3%, and 16 ± 4%, respectively (Fig. S1). The average soil pH (1:2.5 soil: water) is 8.02–8.63 (Fig. S2). The main land-use types include farmland (*Zea mays L.*; *Panicum miliaceum L.*; *Malus pumila*; *Armeniaca vulgaris Lam.*), woodland (*Robinia pseudoacacia L.*; *Pinus tabuliformis Carrière*), shrubland (*Caragana korshinskii*; *Hippophae rhamnoides L.*), and grassland (*Agropyron cristatum*; *Lespedeza davurica*; *Artemisia sacrorum*; *Caragana microphylla*; *Stipa bungeana*; *Artemisia giraldii Pamp.*; *Stipa grandis*; *Heteropappus altaicus*). *Stipa bungeana* is the most widely distributed vegetation.

A stratified random sampling irregular grid was designed by taking into account, terrain condition (Fig. 1b), land-use type (Fig. 1c), and accessibility. The land use map was obtained by vectorizing the aerial photo with 40 cm resolution (available at http://loess.geodata.cn) developed by the Loess Plateau Data Center, National Earth System Science Data Sharing Infrastructure. As for the sampling process, a 300 × 300 m grid was designed for field sampling first. The locations of sampling site were determined to cover as many landscape units of different landforms, terrains, land use types, and vegetation factors as possible. In addition, some sampling sites such as cliffs and deep gullies were not accessible. As a result, an irregular grid was obtained. A global positioning system (GPS) receiver was used to identify the positions of sampling points and a photo camera was used to record the whole sampling process. Field management data were obtained at the site by field observation and farmer interviews. To compare the differences in soil structure distribution and the effects of environmental factors on soil structure at different soil layers, 70 sampling sites (Fig. 1b) were selected to represent the major landscape units at 0–10 cm and 10–20 cm soil layers with three replicates from the same location during June 19th to 26th, 2016. Aluminum containers were used to collect undisturbed soil samples for avoiding soil structural deformation or destruction (Fig. 1d). The soil samples were air-dried afterwards.

2.2. Measurement of aggregate stability

The aggregate stability was measured by using the wet sieving method (Kemper and Rosenau, 1986). Approximately 300 g of air-dried soil samples were sieved on a sieve shaker using a column of sieves at mesh sizes of 5, 2, 1, 0.5 and 0.25 mm. The weights of aggregates remaining on the sieves were recorded and their percentages in the bulk soil were calculated. 50 g of air-dry soil aggregates were prepared based on the above-mentioned percentages. Then, the composed soil samples were sieved for 1 min (30 times) in water (3 replicates). The aggregates with diameters > 5 mm, 5–2 mm, 2–1 mm, 1–0.5 mm and 0.5–0.25 mm were separated again. Then, aggregates remaining on the sieves were transferred into clean beakers. These beakers with soil materials were oven-dried and weighed. Soil aggregate stability was expressed by the mean weight diameter (MWD, mm), percentage of water-stable aggregates that were greater than 0.25 mm ($WSA_{>0.25}$, %), and geometric mean diameter (GMD) by wet sieving. Then, the soil erodibility factors (K factors) were calculated based on the GMD (Li et al., 2016). Equations used in this research include:

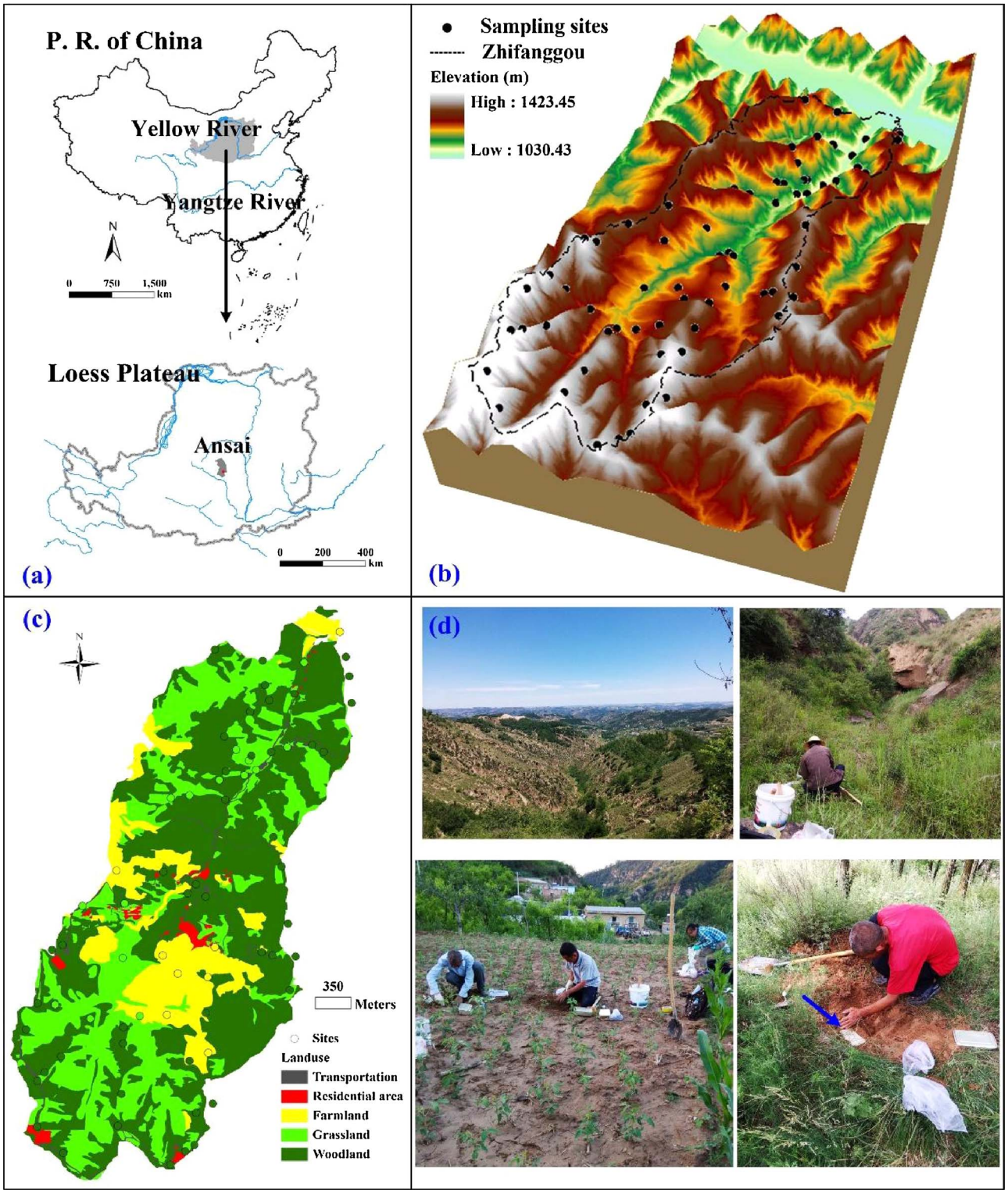

Fig. 1. Study area: (a) Location of Zhifanggou catchment in China; (b) Sampling locations and the digital elevation model; (c) Vectorized land use map from aerial photo with 40 cm resolution; (d) Sampling process.

$$MWD = \sum_{i=1}^{5} \overline{x_i} w_i \quad (1)$$

$$GMD = \exp\left(\sum_{i=1}^{5} w_i \ln \overline{x_i} / \sum_{i=1}^{5} w_i\right) \quad (2)$$

$$K = 7.954 \times \left\{0.0017 + 0.0494 \times \exp\left[-0.5 \times \left(\frac{\log GMD + 1.675}{0.6986}\right)^2\right]\right\} \quad (3)$$

where $\overline{x_i}$ is the mean diameter of i size class (mm), and w_i is the percentage of aggregates in size class i.

2.3. Statistical and geostatistical analyses

Statistical analyses were carried out using Excel and SPSS software. Based on land-use types, the mean and standard deviation for the contents of soil aggregates and their stability were calculated for the entire dataset. Significant differences among different land-use types in soil aggregate stability were tested for LSD (Least Significant Difference) at the 0.05 significance level. MWD and $WSA_{>0.25}$ data were normally distributed, and K factors were unimodal and log-normally distributed.

To confirm the assumption of normality for geostatistical analysis, the K factors were log-transformed and transformed back in GS + 9.0 (Gamma Design Software). Based on the GS + 9.0 software, the spatial variation of soil aggregate stability was analyzed with semivariograms to quantify their spatial structure. Semivariograms, which are based on the theory of regionalized variables, supply input parameters for optimal spatial interpolation (Krige, 1951). There are three major parameters derived from the fitted models of semivariograms, the nugget (C_0), the sill (C_0 + C) and the range (a). The sill (C_0 + C) represents the total variation. The range (a) represents the separation distance at which the measured data become spatially independent beyond a (Cambardella et al., 1994). Then, $C_0/(C_0 + C)$ is considered as a criterion to represent the degree of spatial dependence: very strong (< 25%), moderately strong (25–50%), moderately weak (50–75%), very weak (> 75%), and no spatial dependency (100%) (Cambardella et al., 1994). The common theoretical models of semivariograms include the Spherical, Exponential and Gaussian models (Júnior et al., 2006). Given the importance of the points near the origin in building the kriging weight matrix, repeated comparisons were conducted to select an optimal separation distance in the process of fitting semivariogram models. In this process, not only the maximum range along a certain direction of the study area but the limitation of sample size were considered (Zhang, 2005). Finally, the maximum step length was 1600m in our study. Then, the largest model efficiency (R^2) and the smallest residual were used to determine the best models. The semivariograms can be expressed as:

$$\gamma(h) = \frac{1}{2N(h)} \sum_{i=1}^{N(h)} [z(x_i) - z(x_{i+h})]^2 \quad (4)$$

where $z(x_i)$ and $z(x_{i+h})$ are the values of z at the locations of x_i and x_{i+h}, respectively, $N(h)$ is the number of pair points separated by a distance h (Shukla et al., 2007).

The local spatial dependence of soil aggregate stability was measured using the Geoda software. Local Indicators of Spatial Association (LISA) developed by Anselin (1995) was used to analyze the local spatial autocorrelation and the local clusters of similar behaviors in the spatial arrangement. For each sampling site, the spatial dependence between the sampling site and its neighborhood was then quantified. These relationships included five classes: (i) high-high, high values correlated with high values of its neighbors; (ii) low-low, low values correlated with low values of its neighbors; (iii) low-high relationships; (iv) high-low relationships and (v) no significant spatial dependence.

2.4. Spatial interpolation and accuracy evaluation

Ordinary kriging (OK) and the Inverse distance weighted (IDW) methods were used to map the spatial variability of soil aggregate stability parameters in the Zhifanggou catchment. The spatial analysis module of ArcGIS 9.3 can directly perform the OK and IDW interpolation methods, which has been widely used to obtain the spatial patterns of soil properties (Guan et al., 2017; Mummey et al., 2010; Veihe, 2002). The derivation of IDW parameters is described in the supplementary material. More details about these methods can be found in previous studies (Guan et al., 2017; Liu et al., 2015; Mirzaee et al., 2016).

The prediction accuracy of the MWD, $WSA_{>0.25}$ and K factors was evaluated using leave-one-out cross-validation techniques. The performances of the OK and IDW were compared using four commonly used indices. The statistical measures included the absolute error percentage (AEP), mean absolute error (MAE), root mean square error (RMSE), and determination coefficient (R^2) between the measured and predicted MWD, $WSA_{>0.25}$ and K factors. The AEP, MAE and RMSE are defined as:

$$AEP = \frac{\sum_{i=1}^{n} |P(x_i) - M(x_i)|}{\sum_{i=1}^{n} M(x_i)} \times 100 \quad (5)$$

$$MAE = \frac{1}{n} \sum_{i=1}^{n} [P(x_i) - M(x_i)] \quad (6)$$

$$RMSE = \sqrt{\frac{1}{n} \sum_{i=1}^{n} [P(x_i) - M(x_i)]^2} \quad (7)$$

where $P(x_i)$, $M(x_i)$, and n are predicted values, observed values and the total number of observations, respectively.

3. Results and discussion

3.1. Aggregate stability and soil erodibility under different land uses

The descriptive statistics and significant differences under different land uses are presented in Table 1 for soil aggregate fractions and in Fig. 2 for aggregate stability parameters. Field management data showed that the artificial grassland (*Medicago sativa L*) had been replaced by natural grassland in the process of vegetation restoration. Table 1 shows that the percentage of aggregates with diameters of > 5 mm and 5–2 mm in grassland, shrubland and woodland was significantly higher than that in farmland, but it was the opposite case for the aggregates with diameters of 0.5–0.25 mm. There were no significant differences in the aggregates with diameters of 2–1 mm and 1–0.5 mm among different land uses.

Fig. 2 shows that the difference of soil aggregate stability in various

Table 1
Mean value of aggregate size distribution obtained from wet sieving analysis under different land uses (Mean value ± standard error).

Layer (cm)	Land use	Aggregate content (%)				
		> 5 mm	5-2 mm	2-1 mm	1-0.5 mm	0.5-0.25 mm
0–10	Grassland	24.12 ± 10.14 b	7.64 ± 1.56 c	6.03 ± 2.08 a	6.99 ± 2.62 a	6.36 ± 1.95 a
	Shrubland	26.72 ± 10.43 b	7.05 ± 2.72 bc	6.68 ± 3.62 a	7.27 ± 2.26 a	6.92 ± 2.76 a
	Woodland	19.05 ± 10.98 b	5.87 ± 1.67 b	5.02 ± 2.66 a	6.08 ± 3.03 a	6.12 ± 2.04 a
	Farmland	3.17 ± 1.77 a	3.59 ± 1.33 a	4.92 ± 2.83 a	8.99 ± 4.24 a	8.84 ± 2.36 b
10–20	Grassland	26.23 ± 12.71 BC	7.76 ± 3.74 C	5.99 ± 3.32 A	6.29 ± 2.63 A	5.45 ± 1.78 A
	Shrubland	32.23 ± 15.14 C	6.02 ± 1.95 BC	4.76 ± 1.43 A	5.23 ± 2.21 A	4.93 ± 2.02 A
	Woodland	18.35 ± 9.51 B	4.93 ± 1.81 AB	4.41 ± 2.25 A	5.81 ± 3.1 A	5.65 ± 2.17 A
	Farmland	2.22 ± 0.84 A	3.5 ± 2.77 A	4.58 ± 2.62 A	7.85 ± 2.93 A	8.65 ± 2.12 B

Different letters indicate the significant difference of the percentages of aggregate in a certain size under different land uses within soil layers ($P < .05$).

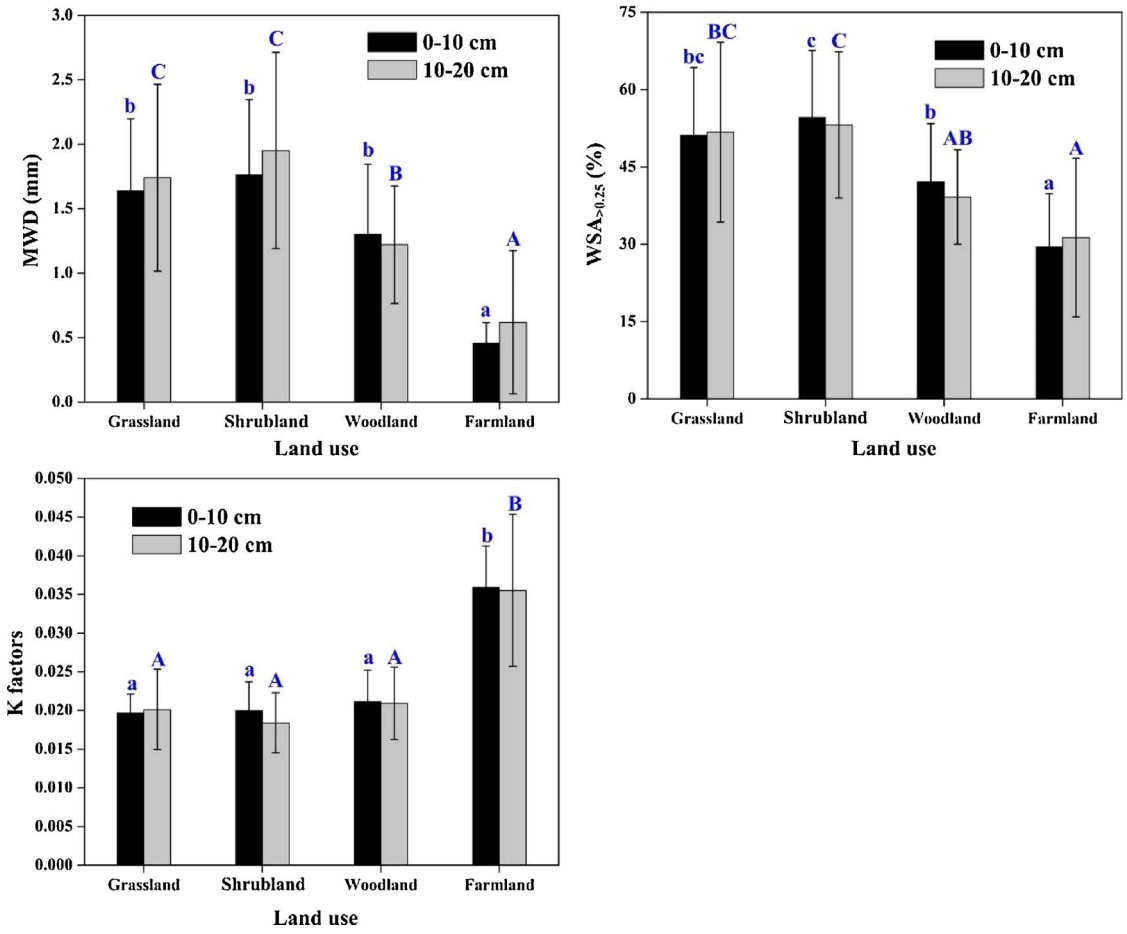

Fig. 2. Comparison of MWD (mm), WSA $_{> 0.25}$ (%) and K factors under different land-use types. Error bars with the same letters are not significantly different by LSD ($P < 0.05$), and different letters indicate significant difference within a depth ($P < 0.05$).

land use types was slightly different between MWD and WSA $_{> 0.25}$. The MWD varied from a minimum of 0.21 mm (farmland) in the 0–10 cm layer to a maximum of 3.23 mm (grassland) in the 10–20 cm layer. It was significantly lower in farmland than in other land types at the 0–10 cm layer, and followed a descending order of shrubland/grassland > woodland > farmland at the 10–20 cm layer. The WSA $_{> 0.25}$ was between 16.41% and 76.61% at 0–10 cm layer, and 14.96% and 83.92% at 10–20 cm layer. There were significant differences between grassland, shrubland, woodland and farmland in WSA $_{> 0.25}$, which was significantly lower in farmland. Meanwhile, there was a significant order of shrubland > woodland > farmland for the 0–10 cm layer, and shrubland/grassland > woodland/farmland for the 10–20 cm layer.

However, K factors behaved just opposite to WSA $_{> 0.25}$ and MWD as far as land uses were concerned, and the higher the K factors were, the lower the aggregate stability was. The K factors ranged from a minimum of 0.0156 (woodland) in 10–20 cm layer to a maximum of 0.0484 (farmland) in 0–10 cm layer. The K factors were significantly higher in farmland than in woodland, shrubland and grassland both for 0–10 cm and 10–20 cm layer. No significant differences were observed between shrubland, grassland and woodland in K factors, but MWD and WSA $_{> 0.25}$ were found to be significantly different among these land types. The soil aggregate stability in 0–10 and 10–20 cm layers showed no significant differences.

The soil aggregate stability of farmland was significantly lower than that of other land-use types at both 0–10 cm and 10–20 cm layers, but its erodibility was the highest among the four land-use types (Fig. 2). Table 1 reveals that farmland had the lowest percentage of large aggregates (> 5 mm and 5–2 mm) and highest percentage of small aggregates (0.5–0.25 mm). These results can be attributed to human impacts, especially plowing. The farmland of LPC has been used for annual ploughing with low organic and inorganic fertilizer inputs, and the soil erosion on the LPC mainly results from poor land use management.

Plowing can destroy the natural soil structure (Greenland and Pereira, 1977) and accelerate the decomposition of SOC (Rovira and Greacen, 1957). Mechanical cultivation causes disruptions of the aggregates and exposes the soil organic matter (SOM) to the soil surface, further accelerating the SOM decomposition. Jastrow (1996) emphasized that SOM plays an important role in binding micro-aggregates and turning them into macro-aggregates. Therefore, these facts will hinder the formation of aggregates or promote the conversion of large aggregates to small ones. On the other hand, mechanical cultivation will destroy the root system and greatly lower the stabilizing effects of root system on soil aggregates, implying a higher vulnerability for soil erosion. Zhang and Horn (2001) found that enhanced microbial decomposition rapidly reduces the SOC content in the plow layer and decreases the aggregate stability due to accelerated soil erosion. Besides, the soil aggregate stability of shrubland, grassland and woodland may benefit from the hydrophobicity of SOC (An et al., 2013). To summarize, the conversion of farmland to woodland, shrubland, or grassland can improve the soil structure and soil resistance to erosion. However, full consideration should be given to the balance between the "Grain for Green" project and the demand of food supply.

The aggregate stability in shrubland and grassland was much higher than that in woodland (Fig. 2). It is in agreement with the results found by An et al. (2013) and Xu (2003), who also obtained similar results in the LPC. Given that SOM and its biological origin are the primary and

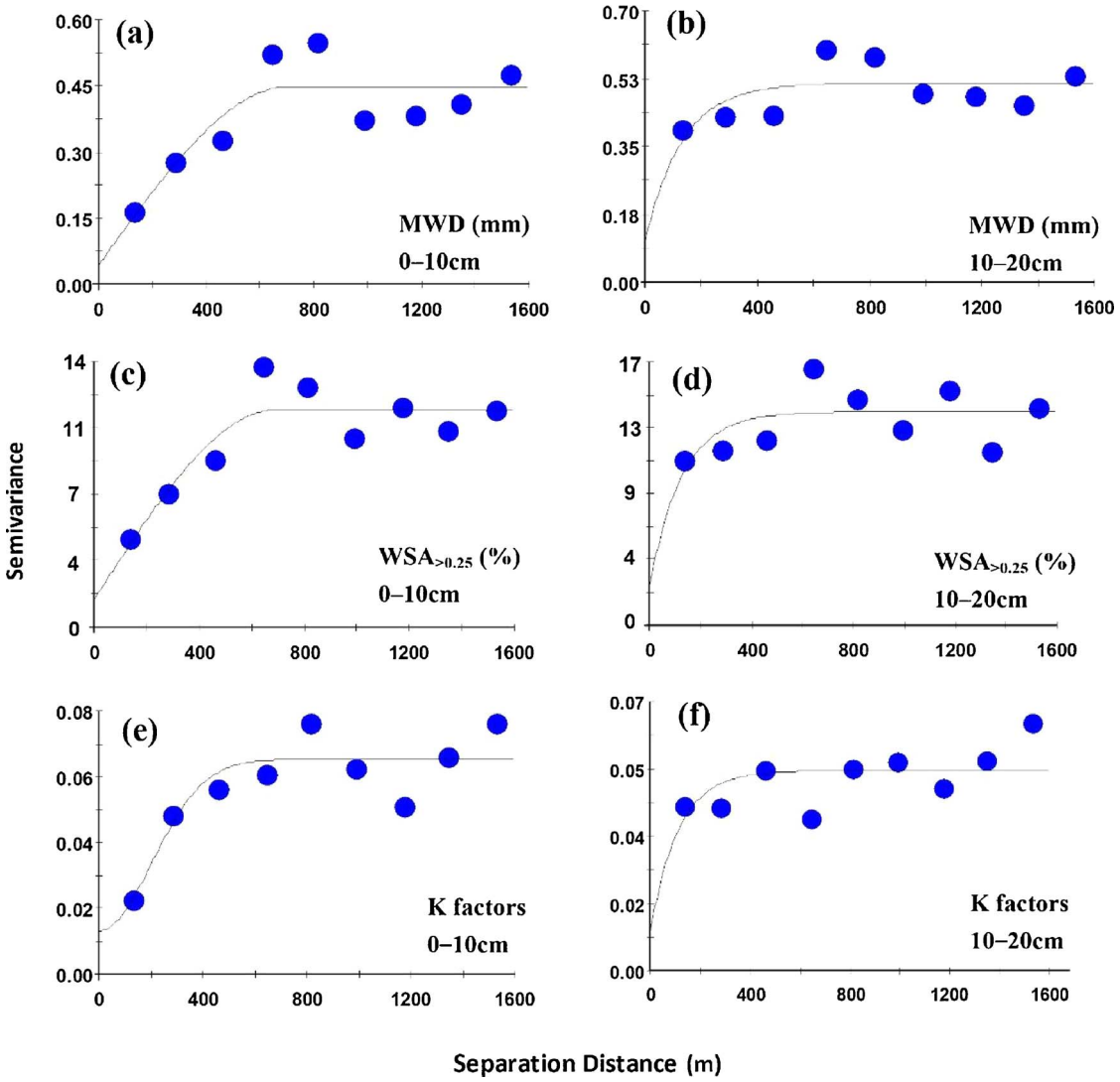

Fig. 3. Experimental semivariograms and the best fitted models for MWD (mm), WSA $_{>0.25}$ (%) and K factors at different soil layers. (a) MWD_0–10 cm, (b) MWD_10–20 cm, (c) WSA $_{>0.25}$_0–10 cm, (d) WSA $_{>0.25}$_10–20 cm, (e) K factors_0–10 cm, (f) K factors_10–20 cm. Their parameters are given in Table 2.

important factors for aggregate stability (Peng et al., 2015), this result may be due to the higher SOM content in the shrubland and grassland than in woodland. As described by Zhang (2012), the SOM contents followed a descending order of shrubland > grassland > woodland > farmland at both 0–10 cm and 10–20 cm layers. The reason is that *Robinia pseudoacacia L.* is the main vegetation type in the woodland of the Zhifanggou catchment (Fig. S3), which can lead to a decrease of SOM at 0–30 cm layer (the root distribution layer) (Zhang et al., 2009). The soil water and mineral assimilation of *Robinia pseudoacacia L.* root can change the soil local environment, leading to the decrease of SOM content and microbial populations and microbial density (Russell et al., 2007; Vesterdal et al., 2002; Zhang et al., 2009).

3.2. Spatial dependence and local spatial autocorrelation analysis

The semivariograms are presented in Fig. 3 and their parameters are shown in Table 2. Spherical, Exponential, and Gaussian models were proved to be the best-fit models in describing the spatial variability of aggregate stability with R^2 varying from 0.20 to 0.82. The fitting effects of kriging methods based on the present semivariograms are already optimal compared with the other models (Table 2 and Table S1). Only for the Spherical model, there is a clear transition to the plateau, and Exponential and Gaussian models do not have a finite range value (Kreba et al., 2017). For facilitating analysis, the points at the position with 95% of $C_0 + C$ will be set as the transition and $C_0 + C$ is considered as the sill of models (Webster, 1985). Table 2 implies that the degree of spatial dependence decreased for the three parameters with increasing soil depth. Each semivariogram was the basis for interpretation of the corresponding parameters by OK method (Table 3).

The nugget values were the variations resulting from experimental errors or the random factors with a scale smaller than the sampling scale. In this study, nugget values were 0.04 and 0.10 for MWD, 1.43 and 2.44 for WSA $_{>0.25}$, and 0.0130 and 0.0098 for K factors in 0–10 and 10–20 cm layers, respectively (Table 2). These low values indicate small sampling errors or random variabilities. The sill represents the total variance, and the sill values were also low for MWD, WSA $_{>0.25}$ and K factors. When the distance is beyond the range, the variables will be considered as not correlated. MWD, WSA $_{>0.25}$ and K factors had a larger range of spatial autocorrelation in 0–10 cm layer than in 10–20 cm layer. The lowest range value (336 m) was found for K factors at 10–20 cm layer, indicating a maximal heterogeneity and a lowest spatial dependence.

$C_0/(C_0 + C)$ represents the degree of spatial dependence and the detailed description is provided in Section 2.3. Soil intrinsic factors, such as soil parent material, soil texture, topography and vegetation, contribute to the “very strong” spatial dependence. On the contrary,

Table 2
Semivariance models and their parameters for MWD (mm), $WSA_{>0.25}$ (%) and K factors at different soil layers.

Parameter	Layers (cm)	Models	C_0	$C_0 + C$	$C_0/(C_0 + C)$ (%)	a (m)	R^2
MWD (mm)	0–10	Spherical	0.04	0.45	9.13	714	0.74
	10–20	Exponential	0.10	0.51	19.49	390	0.37
$WSA_{>0.25}$ (%)	0–10	Spherical	1.43	11.46	12.48	696	0.82
	10–20	Exponential	2.44	13.78	17.71	381	0.32
K factors	0–10	Gaussian	0.0130	0.0653	19.91	495	0.76
	10–20	Exponential	0.0098	0.0520	18.85	336	0.20

C_0 – Nugget; $C_0 + C$ – Sill; $C_0/(C_0 + C)$ – Nugget/Sill, the spatial dependence degree; a – Range; R^2 – Model efficiency; MWD – mean weight-diameter; $WSA_{>0.25}$ – percentage of water-stable aggregates that were greater than 0.25 mm; K factors – soil erodibility factor k.

Table 3
Cross-validation indices of ordinary kriging (OK) for soil aggregate stability and erodibility.

Parameter	Layers (cm)	AEP (%)	MAE	RMSE	R^2
MWD (mm)	0–10	34.12	0.39	0.53	0.402
	10–20	39.08	0.54	0.66	0.179
$WSA_{>0.25}$ (%)	0–10	20.71	9.09	12.27	0.377
	10–20	25.14	11.03	14.09	0.257
K factors	0–10	21.03	0.0049	0.0071	0.153
	10–20	22.54	0.0050	0.0065	0.075

AEP – absolute error percentage; MAE – mean absolute error; RMSE – root mean square error; R^2 – determination coefficient; MWD – mean weight-diameter; $WSA_{>0.25}$ – percentage of water-stable aggregates that were greater than 0.25 mm; K factors – soil erodibility factor k.

soil extrinsic factors, such as fertilization and cultivation practices, are repsonsible for the “moderately weak” and “very weak” spatial dependence (Wang et al., 2009). Accordingly, “moderately strong” spatial dependence can be attributed to both intrinsic and extrinsic factors. In this study, the nugget/sill ratios of MWD and $WSA_{>0.25}$ ranged from 9.13% to 17.71%, indicating a very strong spatial dependence at both 0–10 and 10–20 cm layers, which is mainly determined by soil intrinsic factors. Besides, the nugget/sill ratios of K factors were 19.91% and 18.85% and K factors had lowest range values, indicating a very strong to moderately strong spatial dependence, which is controlled by the interactions of intrinsic and extrinsic factors. These results are different from those reported by Xu (2003), who concluded that the spatial heterogeneity of aggregate satbility mainly resulted from the land use change (97%) in Zhifanggou catchment. In initial stage of restoration, the soil structure is mainly affected by human impacts, but in the later stage of restoration, it is mainly controlled by soil properties, topography and vegetation. In addition, poor land use management is an important factor responsible for the soil erosion on the LPC. Hence, human impacts, such as tillage, should not be ignored as well, especially for soil erodibility K factors.

Fig. 4 shows the clear spatial structures of MWD, $WSA_{>0.25}$ and K factors according to LISA analyses. The five distinct classes are: (i) in red, high values correlated with high values of its neighbors (high-high); (ii) in blue, low values correlated with low values of its neighbors (low-low); (iii) in violet, a low-high relationship (low-high); (iv) in pink, a high-low relationship (high-low); and finally (v) white circles, which show places with no significant spatial dependence. For these three parameters, one significant cluster emerged in the southeast part of Zhifanggou catchment around the farmland of Siyaoxian village (Fig. 1c and Fig. 4). There are large areas of terraces with intensive agricultural practices (Fig. S4). It is the low-low region for MWD and $WSA_{>0.25}$ and high-high region for K factors, which further proves the relation of a particularly low aggregate stability and high erodibility to intensive agricultural practices. But for MWD and $WSA_{>0.25}$, many low-low relationships were located in the woodland neighboring farmland with a revegetation duration of 17 years. According to the sampling information, these woodland areas had steep slopes (with an average of 21°) (Figs. S5 and S6). Dong (2011) also showed that the locust forest with a steep slope had a low aggregate stability in the LPC. Moreover, the large amount of sheep dung on the ground indicated intensive grazing in this region. Grazing can significantly reduce the aggregate stability. However, high-low and low-high relationships were scattered in the transition zones of revegetation duration, topography and land use, implying complex interactions between these factors.

As for MWD and $WSA_{>0.25}$, they had a similar spatial distribution of high-high relationships in 0–10 cm layer, mainly in woodland with an average revegetation duration of 18 years, which may be due to the largest distribution of woodland (56.2%) in Zhifanggou catchment. The high-high relationships of $WSA_{>0.25}$ were also located in shrubland and grassland with an average slope of 14° and revegetation duration of 19 years (Fig. S6). It is interesting to note that one high-high relationship (northern part of Zhifanggou catchment) in 0–10 cm soil layer and low-high relationship in 10–20 cm soil layer were located in shrubland with a one-year revegetation duration. This site is surrounded by woodland with a revegetation duration of more than 10 years (an average of 23.4 years) and a favorable soil structure. It has a high-high relationship with those woodlands at 0–10 cm soil layer, indicating that the conversion of farmland to shrubland has a stronger positive effect on the surface aggregates than on the sub-surface aggregates after a short-term soil restoration. In the soil aggregate fractions, aggregates with sizes of > 5 mm accounted for 31.5% of $WSA_{>0.25}$ in 0–10 cm layer and 18.9% in 10–20 cm layer, which emphasizes the better soil structure in 0–10 cm than in 10–20 cm layer. In addition, there were mainly high-high relationships at 0–10 cm (9 points) and low-low relationships at 10–20 cm layer (6 points), further indicating the positive effects of artificial forest and grassland on the formation of surface aggregates. In Fig. 4, high-high and high-low relationships of MWD and $WSA_{>0.25}$ indicated the good soil structure in these areas. The areas with low-low and low-high relationships were prone to soil erosion with poor soil structural stability. The K factors had the opposite results.

Based on the aforementioned analysis, the aggregate stability and soil erodibility are comprehensively influenced by land uses, vegetation types, revegetation duration, topography, plowing, and grazing intensity at the catchment scale. Their effects on soil structure are different in two soil layers at spatial scale. In general, LISA analysis can further explore the spatial influencing factors of aggregate stability and erodibility from the local spatial patterns, which demonstrates the effectiveness of this method in analyzing the local spatial patterns of soil properties. In addition, soil erodibility factors are an effective indicator to represent the spatial pattern of soil structure.

3.3. Spatial patterns of aggregate stability and erodibility

Spatial distribution maps were generated to comparatively analyze the differences of OK and IDW for the interpolation of MWD, $WSA_{>0.25}$ and K factors in different soil layers (Figs. 5–7 and Figs. S7–S9). In addition, the artificial impervious surface (Fig. 1c) was not taken into account in the two methods, such as the villages, roads and diggings. It was found that the three parameters had a large spatial variability over the catchment. There were no remarkable differences in the spatial

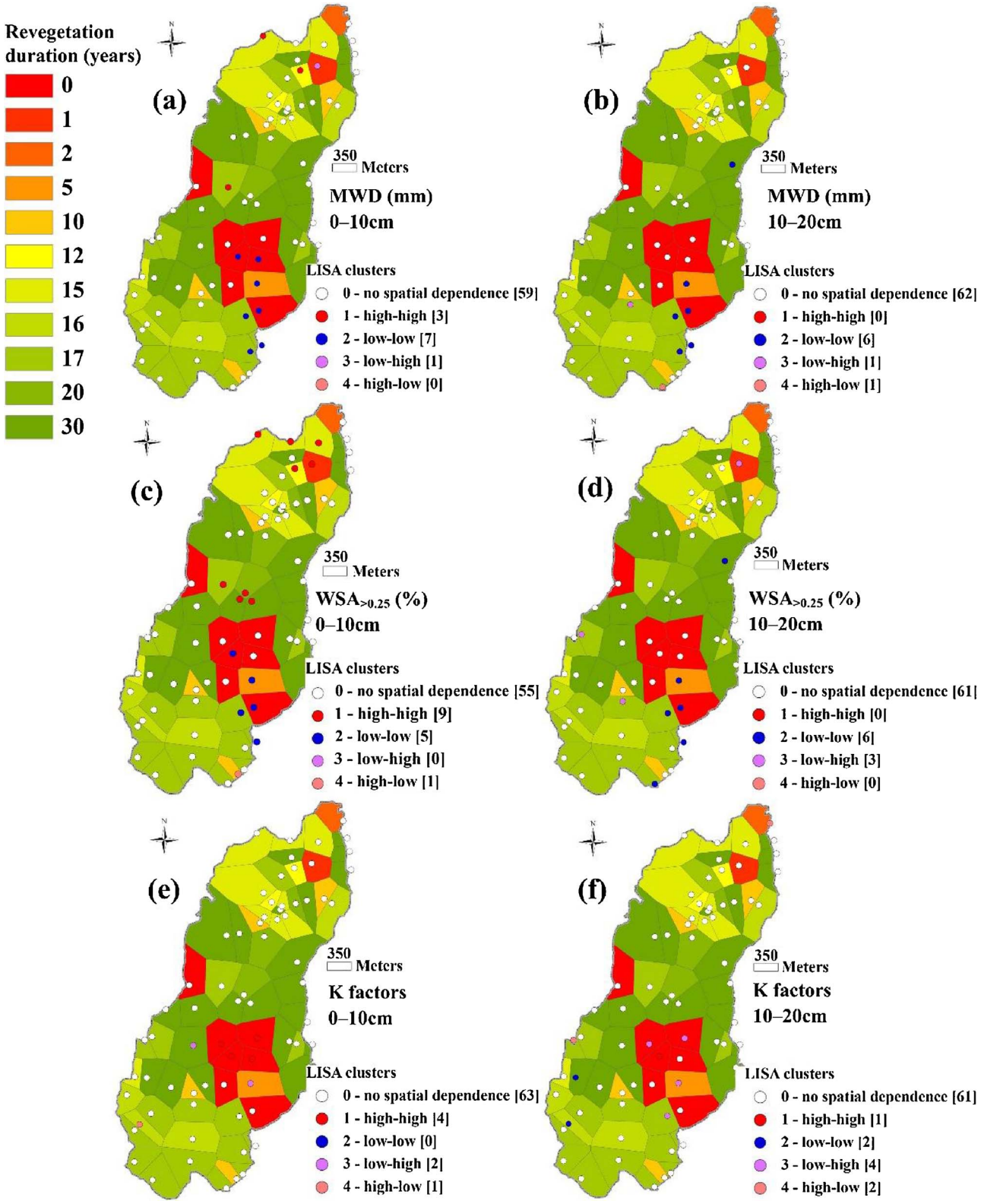

Fig. 4. Cluster map of the Local Indices of Spatial Association (LISA) for MWD (mm), $WSA_{>0.25}$ (%) and K factors at different soil layers. (a) MWD_0–10 cm, (b) MWD_10–20 cm, (c) $WSA_{>0.25}$_0–10 cm, (d) $WSA_{>0.25}$_10–20 cm, (e) K factors_0–10 cm, (f) K factors_10–20 cm. Results are significant at $p = .05$ (999 permutations). The background shows the distribution of revegetation duration (years). It was obtained by building Voronoi diagram based on the sampling sites.

distribution of MWD, $WSA_{>0.25}$ and K factors at different soil layers between OK and IDW interpolation, proving the suitability of OK and IDW. Generally, the MWD and $WSA_{>0.25}$ spatial distribution patterns were very similar between the two methods, and the results only differed in the details. The spatial distributions showed that areas with low MWD, low $WSA_{>0.25}$ and high K factors were mostly located around the farmland in the southeast part of Zhifanggou catchment (Figs. 5–7 and Figs. S7–S9), which is in agreement with the LISA maps (Fig. 4). Then, based on the spatial maps of LISA analysis, land use, 3D-elevation, and revegetation duration, spatial overlay analysis was used to

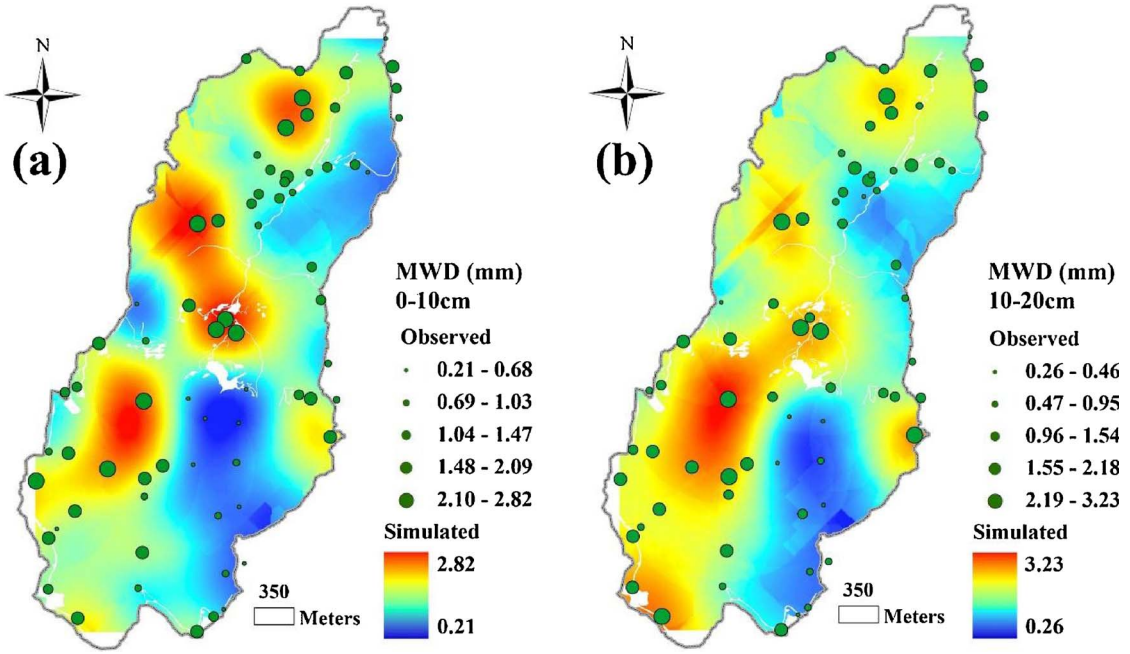

Fig. 5. Spatial interpolation of MWD (mm) using OK at different soil layers. (a) 0–10 cm, (b) 10–20 cm.

explore the influencing factors of the three parameters.

The highest MWD and $WSA_{>0.25}$ were mainly found in the central part and southwest of the map, which is similar to the distribution of revegetation duration of more than 17 years. Besides, they were more widespread in 0–10 cm layer than in 10–20 cm layer (Figs. 5 and 6, Figs. S7 and S8 and S10a, b), further indicating the significant impact of woodland, shrubland and grassland on the aggregate stability in the surface layer. Moreover, the lowest MWD and $WSA_{>0.25}$ were mainly distributed around the Siyaoxian's farmland and the northeast of the maps. They were more widely distributed in 0–10 cm soil layer (Figs. 5 and 6, Figs. S7 and S8 and S10a, b), indicating that cultivation has more significant impacts on aggregate stability in 0–10 cm than in 10–20 cm layer. As mentioned in Section 3.2, the soil aggregate fractions in areas with short-term revegetation contained a highest proportion of aggregates with sizes of 1–0.25 mm. That is the reason why the areas with high value of $WSA_{>0.25}$ (Fig. 6, Figs. S8 and S10b) were more extensive than that of MWD (Fig. 5, Figs. S7 and S10a).

Conversely, the highest K factors were mainly found in farmland areas or areas with a one-year revegetation duration (Fig. 7, Fig. S9 and Fig. 1c). They were more widespread in 0–10 cm layer than in 10–20 cm layer (Fig. 7, Figs. S9 and S10c), indicating that human impact on soil erodibility is more significant in 0–10 cm than in 10–20 cm layer. In addition, it is noteworthy that the farmland areas in the midwest of Zhifanggou catchment had better soil structure than those in the southeast, which is probably due to the flat terrain in the midwest and complex terrain in the southeast. The farmlands in the southeast are surrounded by residential areas, which further increases the intensity of human disturbance (Fig. S4). The low value of K factors was mainly

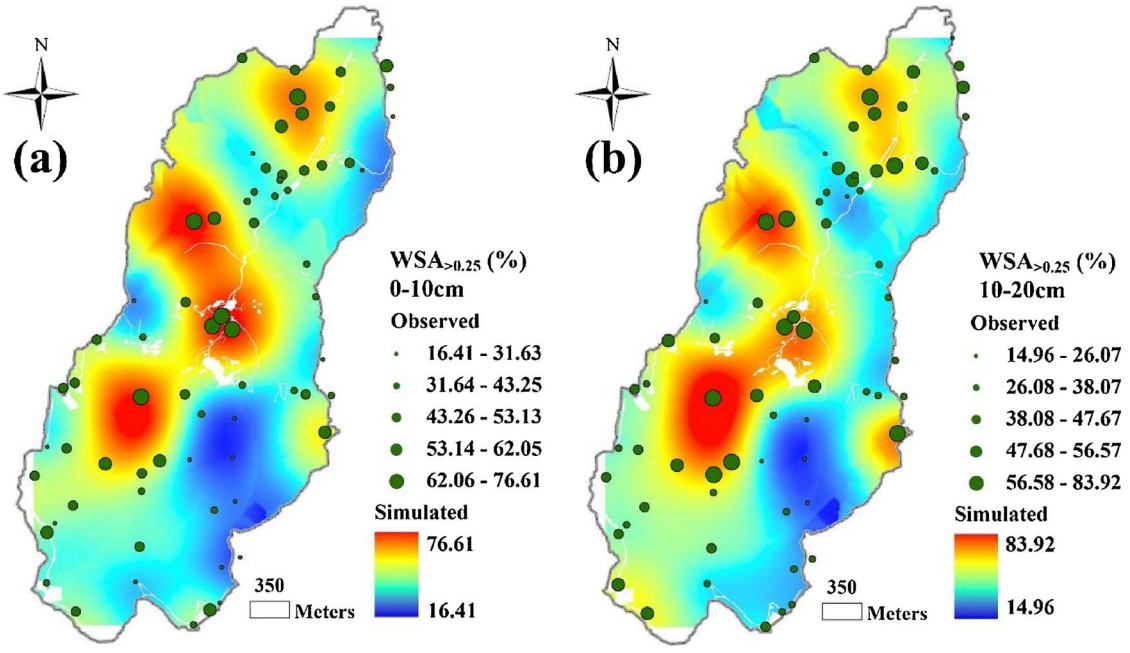

Fig. 6. Spatial interpolation of $WSA_{>0.25}$ (%) using OK at different soil layers. (a) 0–10 cm, (b) 10–20 cm.

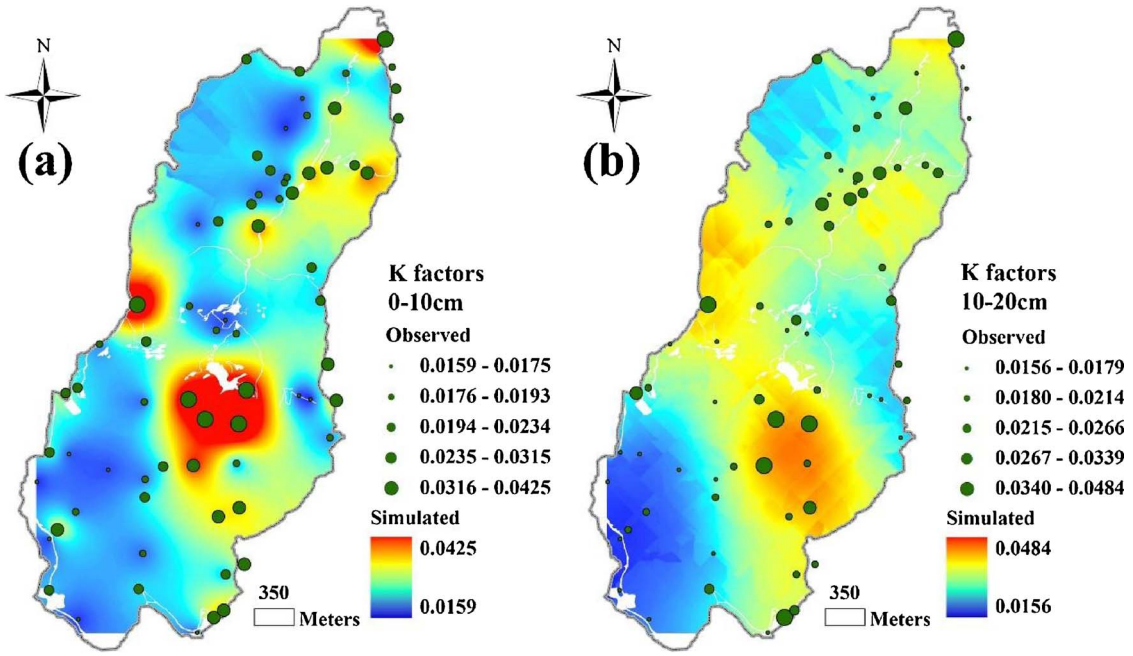

Fig. 7. Spatial interpolation of K factors using OK at different soil layers. (a) 0–10 cm, (b) 10–20 cm.

located in woodland, shrubland and grassland (Fig. 7, Figs. S9 and S10c), and it was more widely distributed in 0–10 cm layer, revealing the significant improvement of soil erosion resistance in the surface layer by woodland, shrubland and grassland.

The abovementioned results further confirm the different spatial structures of MWD, $WSA_{>0.25}$ and K factors. They are affected by the synergistic effects of land use, revegetation duration and topography. Our results indicate that the woodland, grassland and shrubland have significantly improved MWD and $WSA_{>0.25}$ and decreased K factors changes compared to that of farmland, and the improving effects are largely dependent on the topography, vegetation factors and land use patterns. However, the afforestation in the Zhifanggou catchment did not take those factors into account previously (such as the plantation of *Robinia pseudoacacia L.*). Therefore, in the "Grain for Green" project, measures should be adjusted according to different local topographies and conditions to improve soil structure in different areas, rather than adopting unified management across the whole catchment. For example, more farming practices can be conducted in the midwest areas with flat terrain to ensure the basic farmland protection, and farmland in the southeast areas with steep terrain should be returned to forest or utilized in terraced farming to reduce soil erosion, which is also consistent with the 5-year fallow policy of the government. Moreover, it is not suitable to plant trees in steep slope areas.

4. Conclusions

Geostatistical methods are suitable for assessing spatial variability of aggregate stability and soil erodibility in a small catchment. There is a downward trend for MWD and $WSA_{>0.25}$ and an upward trend for K factors from surface to subsurface soil, although they show some variations in some regions. The variability of the three parameters is high in the two soil layers. Land-use type has remarkable effects on MWD, $WSA_{>0.25}$ and K factors. The mean MWD and $WSA_{>0.25}$ follow the order of shrubland/grassland/woodland > farmland at both 0–10 and 10–20 cm soil depths, while it is the opposite case for K factors. Vegetation factors and slope have significant influence on soil structure. As for the main vegetation type in the woodland of the Zhifanggou catchment, *Robinia pseudoacacia L.* can lead to a decrease of aggregate stability in the 0–20 cm soil layer. Aggregate stability increases with increasing revegetation duration but with decreasing slope. The semivariograms and spatial interpolation revealed that the aggregate stability and soil erodibility of the small catchment are comprehensively influenced by land use, vegetation factor, and topography. LISA analysis further highlighted the factors affecting the soil structure and erodibility in the small catchment scale from the local spatial characteristics, which promotes the analysis to a higher level compared with semivariograms.

The differences between OK and IDW indicate that they have similar performance for MWD, $WSA_{>0.25}$, and K factors in most regions of the catchment, except for the areas with the highest and lowest values. Sampling sites at high density are hardly available to interpolate the spatial pattern of soil aggregate stability in an area as large as the LPC. The spatial structure of aggregate stability is always associated with the spatial structures of environmental variables like land use, topography, and vegetation. The low correlation between the predicted and measured data suggest that a better prediction methodology should be developed to improve the accuracy of spatial interpolation of MWD, $WSA_{>0.25}$ and K factors, including both intrinsic and extrinsic factors. Estimating the contributions of intrinsic and extrinsic factors to the spatial variability of MWD, $WSA_{>0.25}$ and K factors will be further conducted based on the results of this study.

Acknowledgments

This investigation supported by National Natural Science Foundation of China (No. 41330852) and the National Key Basic Research Program of China (No. 2015CB150504). We also like to thank Li Zhang, Zhenglun Yang and Tiexiong Gong for sampling and thank "Loess Plateau Data Center, National Earth System Science Data Sharing Infrastructure, National Science & Technology Infrastructure of China (http://loess.geodata.cn)" for the aerial photo with 40 cm resolution. Mr. Zuoxiong Liu was acknowledged to polish the language.

Appendix A. Supplementary data

Supplementary material related to this article can be found, in the online version, at doi:https://doi.org/10.1016/j.still.2018.01.012.

References

Algayer, B., Le Bissonnais, Y., Darboux, F., 2014a. Short-term dynamics of soil aggregate stability in the field. Soil Sci. Soc. Am. J. 78, 1168–1176.

Algayer, B., Wang, B., Bourennane, H., Zheng, F., Duval, O., Li, G., Le Bissonnais, Y., Darboux, F., 2014b. Aggregate stability of a crusted soil: differences between crust and sub-crust material, and consequences for interrill erodibility assessment. An example from the Loess Plateau of China. Eur. J. Soil Sci. 65, 325–335.

Amezketa, E., 1999. Soil aggregate stability: A review. J. Sustain. Agric. 14, 83–151.

An, S.S., Darboux, F., Cheng, M., 2013. Revegetation as an efficient means of increasing soil aggregate stability on the Loess Plateau (China). Geoderma 209, 75–85.

Annabi, M., Raclot, D., Bahri, H., Bailly, J.S., Gomez, C., Le Bissonnais, Y., 2017. Spatial variability of soil aggregate stability at the scale of an agricultural region in Tunisia. Catena 153, 157–167.

Anselin, L., 1995. Local indicators of spatial association—LISA. Geogr. Anal. 27, 93–115.

Barik, K., Aksakal, E.L., Islam, K.R., Sari, S., Angin, I., 2014. Spatial variability in soil compaction properties associated with field traffic operations. Catena 120, 122–133.

Cambardella, C.A., Moorman, T.B., Novak, J.M., Parkin, T.B., Karlen, D.L., Turco, R.F., Konopka, A.E., 1994. Field-scale variability of soil properties in Central Iowa soils. Soil Sci. Soc. Am. J. 58, 1501–1511.

Cantón, Y., Solé-Benet, A., Asensio, C., Chamizo, S., Puigdefábregas, J., 2009. Aggregate stability in range sandy loam soils relationships with runoff and erosion. Catena 77, 192–199.

Castrignanò, A., Goovaerts, P., Lulli, L., Bragato, G., 2000. A geostatistical approach to estimate probability of occurrence of tuber melanosporum in relation to some soil properties. Geoderma 98, 95–113.

Castrignanò, A., Stelluti, M., 1999. Fractal geometry and geostatistics for describing the field variability of soil aggregation. J. Agric. Eng. Res. 73, 13–18.

Cooperative Research Group on Chinese Soil Taxonomy (CRGCST), 2001. Chinese Soil Taxonomy, 3rd edition. Science Press, Beijing.

Deng, C., Teng, X., Peng, X., Zhang, B., 2014. Effects of simulated puddling intensity and pre-drying on shrinkage capacity of a paddy soil under long-term fertilization. Soil Tillage Res. 140, 135–143.

Dong, L.L., 2011. Characteristics of soil water stable aggregates under different land-use types. Scientia Silvae Sinicae 47, 95–100 (in Chinese).

Freitas, A.S., Pozza, E.A., Alves, M.C., Coelho, G., Rocha, H.S., Pozza, A.A.A., 2015. Spatial distribution of Yellow Sigatoka leaf spot correlated with soil fertility and plant nutrition. Precis. Agric. 17, 93–107.

Gallardo-Carrera, A., Léonard, J., Duval, Y., Dürr, C., 2007. Effects of seedbed structure and water content at sowing on the development of soil surface crusting under rainfall. Soil Tillage Res. 95, 207–217.

Greenland, D., Pereira, H., 1977. Soil damage by intensive arable cultivation: temporary or permanent? Philos. Trans. R: Soc. Lond. Ser. B. 281, 193–208.

Guan, F., Xia, M., Tang, X., Fan, S., 2017. Spatial variability of soil nitrogen, phosphorus and potassium contents in Moso bamboo forests in Yong'an City, China. Catena 150, 161–172.

Hajabbasi, M.A., Hemmat, A., 2000. Tillage impacts on aggregate stability and crop productivity in a clay-loam soil in central Iran. Soil Tillage Res. 56, 205–212.

IUSS Working Group, 2014. World Reference Base for Soil Resources 2014. International Soil Classification System for Naming Soils and Creating Legends for Soil Maps. World Soil Resources Reports No. 106. FAO, Rome.

Júnior, V.V., Carvalho, M.P., Dafonte, J., Freddi, O.S., Vidal Vázquez, E., Ingaramo, O.E., 2006. Spatial variability of soil water content and mechanical resistance of Brazilian ferralsol. Soil Tillage Res. 85, 166–177.

Jastrow, J., 1996. Soil aggregate formation and the accrual of particulate and mineral-associated organic matter. Soil Biol. Biochem. 28, 665–676.

Jastrow, J.D., Miller, R.M., 1997. Soil aggregate stabilization and carbon sequestration: feedbacks through organomineral associations. In: Lal, R., Kimble, J.M., Follett, R.F., Stewart, B.A. (Eds.), Soil Processes and the Carbon Cycle. CRC Press, Boca Raton, pp. 207–223.

Kemper, W.D., Rosenau, R.C., 1986. Aggregate stability and size distribution. Methods of Soil Analysis, Part 1. Physical and Mineralogical Methods. Agronomy Monograph No. 9. Soil Science Society of America, pp. 425–442.

Kreba, S.A., Wendroth, O., Coyne, M.S., Walton, R., 2017. Soil gas diffusivity, air-filled porosity, and Pore continuity: land use and spatial patterns. Soil Sci. Soc. Am. J. 81, 477–489.

Krige, D.G., 1951. A statistical approach to some basic mine valuation problems on the witwatersrand. J. South Afr. Inst. Min. Metall. 52, 119–139.

Langella, G., Basile, A., Bonfante, A., Mileti, F.A., Terribile, F., 2016. Spatial analysis of clay content in soils using neurocomputing and pedological support: a case study of Valle Telesina (South Italy). Environ. Earth Sci. 75.

Li, Y.Y., Liu, L., An, S.S., Zeng, Q.C., Li, X., 2016. Research on the effect of vegetation and slope aspect on the stability and erodibility of soil aggregate in Loess hilly region based on Le Bissonnais method. J. Nat. Resour. 31, 287–298 (in Chinese).

Liu, S., An, N., Yang, J., Dong, S., Wang, C., Yin, Y., 2015. Prediction of soil organic matter variability associated with different land use types in mountainous landscape in southwestern Yunnan province, China. Catena 133, 137–144.

Lynch, J., Bragg, E., 1985. Microorganisms and soil aggregate stability. Adv. Soil Sci. 2, 133–171.

Mirzaee, S., Ghorbani-Dashtaki, S., Mohammadi, J., Asadi, H., Asadzadeh, F., 2016. Spatial variability of soil organic matter using remote sensing data. Catena 145, 118–127.

Mummey, D.L., Clarke, J.T., Cole, C.A., O'Connor, B.G., Gannon, J.E., Ramsey, P.W., 2010. Spatial analysis reveals differences in soil microbial community interactions between adjacent coniferous forest and clearcut ecosystems. Soil Biol. Biochem. 42, 1138–1147.

Nielsen, D., Alemi, M.H., 1989. Statistical opportunities for analyzing spatial and temporal heterogeneity of field soils. Plant. Soil 115, 261–272.

O'Brien, S.L., Jastrow, J.D., 2013. Physical and chemical protection in hierarchical soil aggregates regulates soil carbon and nitrogen recovery in restored perennial grasslands. Soil Biol. Biochem. 61, 1–13.

Ou, Y., Rousseau, A.N., Wang, L., Yan, B., 2017. Spatio-temporal patterns of soil organic carbon and pH in relation to environmental factors—a case study of the black soil region of Northeastern China. Agric. Ecosyst. Environ. 245, 22–31.

Peng, X., Yan, X., Zhou, H., Zhang, Y., Sun, H., 2015. Assessing the contributions of sesquioxides and soil organic matter to aggregation in an ultisol under long-term fertilization. Soil Tillage Res. 146, 89–98.

Rovira, A., Greacen, E., 1957. The effect of aggregate disruption on the activity of microorganisms in the soil. Aust. J. Agric. Res. 8, 659–673.

Russell, A.E., Raich, J.W., Valverde-Barrantes, O., Fisher, R., 2007. Tree species effects on soil properties in experimental plantations in tropical moist forest. Soil Sci. Soc. Am. J. 71, 1389–1397.

Shi, Z.H., Ai, L., Fang, N.F., Zhu, H.D., 2012. Modeling the impacts of integrated small watershed management on soil erosion and sediment delivery: a case study in the Three Gorges Area, China. J. Hydrol. 438–439, 156–167.

Shukla, M.K., Lal, R., VanLeeuwen, D., 2007. Spatial variability of aggregate-associated carbon and nitrogen contents in the reclaimed minesoils of Eastern Ohio. Soil Sci. Soc. Am. J. 71, 1748–1757.

Siqueira, D.S., Marques, J., Pereira, G.T., 2010. The use of landforms to predict the variability of soil and orange attributes. Geoderma 155, 55–66.

Veihe, A., 2002. The spatial variability of erodibility and its relation to soil types: a study from northern Ghana. Geoderma 106, 101–120.

Vesterdal, L., Ritter, E., Gundersen, P., 2002. Change in soil organic carbon following afforestation of former arable land. For. Ecol. Manage. 169, 137–147.

Wang, B., Liu, G.B., Xue, S., Zhu, B.B., 2011. Changes in soil physico-chemical and microbiological properties during natural succession on abandoned farmland in the Loess Plateau. Environ. Earth. Sci. 62, 915–925.

Wang, Y., Zhang, X., Huang, C., 2009. Spatial variability of soil total nitrogen and soil total phosphorus under different land uses in a small watershed on the Loess Plateau, China. Geoderma 150, 141–149.

Wang, Z., Hu, Y., Wang, R., Guo, S., Du, L., Zhao, M., Yao, Z., 2017. Soil organic carbon on the fragmented Chinese Loess Plateau: combining effects of vegetation types and topographic positions. Soil Tillage Res. 174, 1–5.

Wang, Z., Shi, W., 2017. Mapping soil particle-size fractions: a comparison of compositional kriging and log-ratio kriging. J. Hydrol. 546, 526–541.

Webster, R., 1985. Quantitative spatial analysis of soil in the field. Advances in Soil Science. Springer, pp. 1–70.

Xu, M.X., 2003. Soil Quality Evolvement Mechanism in the Process of Ecosystem Restoration and Its Management in the Hilly Loess Plateau. Northwest A&F University (in Chinese).

Zhang, B., Horn, R., 2001. Mechanisms of aggregate stabilization in ultisols from subtropical China. Geoderma 99, 123–145.

Zhang, J., Su, Y., Kang, Y., Xu, X., Qin, Y., 2009. Carbon sequestration of young Robinia pseudoacacia plantation in Loess Plateau. Chin. J. Appl. Ecol. 20, 2911–2916 (in Chinese).

Zhang, R., 2012. Spatial Distribution of Soil Inorganic Carbon Density, Stock and Its Affecting Factors in the Loess Plateau. Institute of Soil and Water Conservation, CAS & MWR (in Chinese).

Zhang, R.D., 2005. Theory and Application of Spatial Variability. Science Press, Beijing (in Chinese).

Zhang, X., Zhang, L., Zhao, J., Rustomji, P., Hairsine, P., 2008. Responses of streamflow to changes in climate and land use/cover in the Loess Plateau, China. Water Resour. Res. 44, 2183–2188.

Zhang, Z.H., 1991. Soil erosion processes in the Loess Plateau of Northwestern China. GeoJournal 24, 195–200.

Zhao, D., Xu, M., Liu, G., Yao, X., Tuo, D., Zhang, R., Xiao, T., Peng, G., 2017. Quantification of soil aggregate microstructure on abandoned cropland during vegetative succession using synchrotron radiation-based micro-computed tomography. Soil Tillage Res. 165, 239–246.

Zhao, W., Zhang, R., Huang, C.Q., Wang, B.Q., Cao, H., Koopal, L.K., Tan, W.F., 2016. Effect of different vegetation cover on the vertical distribution of soil organic and inorganic carbon in the Zhifanggou Watershed on the loess plateau. Catena 139, 191–198.

Zhou, D., Zhao, S., Zhu, C., 2012. The grain for green project induced land cover change in the Loess Plateau: a case study with Ansai County, Shanxi Province, China. Ecol. Indic. 23, 88–94.

Zhou, Z.C., Shangguan, Z.P., Zhao, D., 2006. Modeling vegetation coverage and soil erosion in the Loess Plateau Area of China. Ecol. Model. 198, 263–268.